

Variations in the electrical resistivity of Y_2O_3 -doped ZrO_2 ceramics with microstructural design

This article has been downloaded from IOPscience. Please scroll down to see the full text article.

1994 J. Phys.: Condens. Matter 6 4343

(<http://iopscience.iop.org/0953-8984/6/23/014>)

View [the table of contents for this issue](#), or go to the [journal homepage](#) for more

Download details:

IP Address: 171.66.16.147

The article was downloaded on 12/05/2010 at 18:35

Please note that [terms and conditions apply](#).

Variations in the electrical resistivity of Y_2O_3 -doped ZrO_2 ceramics with microstructural design

Thae-Khapp Kang and Sun-Jae Kim

Hi-Tech Ceramics Team, Korea Atomic Energy Research Institute, PO Box 105 Yusong,
Taejeon 305-600, Korea

Received 22 November 1993, in final form 25 February 1994

Abstract. The change in the electrical resistivity of Y_2O_3 -doped ZrO_2 ceramics with microstructural modification was investigated. Two kinds of ZrO_2 powder containing 8 mol% Y_2O_3 (8Y) and 3 mol% Y_2O_3 (3Y) were used as the raw powders. Six kinds of microstructure were designed: two single-phase specimens (8YS and 3YS) and four mixed-phase specimens (Par, Ser, GG and CC). Using an impedance analyser, the contributions of the structural components, i.e. bulk and boundary, to the electrical resistivity were identified in air up to 750 °C. Microstructures that contained a large phase boundary area revealed a high electrical resistivity. In the low-temperature region, the grain boundaries and/or phase boundaries played important roles in the electrical resistivity while the contribution of the bulk component increased as the temperature increased.

1. Introduction

As a new energy device, solid oxide fuel cells have been widely investigated using ZrO_2 [1, 2]. Thin and homogeneous ZrO_2 films have mostly been produced by tape casting [3, 4] and chemical vapour [5, 6] processes. To reduce the electrical resistivity, fully stabilized ZrO_2 doped with 8 mol% Y_2O_3 (8Y) has mainly been used, but 8Y is very weak in strength. On the other hand, partially stabilized ZrO_2 doped with 3 mol% Y_2O_3 (3Y) shows a somewhat high resistivity, but very high strength and high fracture toughness [7].

Microstructure designs and their relationships with electrical properties have been important research subjects [8, 9]. In order to develop ZrO_2 thin films that have a low electrical resistivity and a high strength, mixed-phase ZrO_2 ceramics with 8Y and 3Y were investigated [10]. In this work, the microstructures of several ZrO_2 ceramics were designed using 8Y and 3Y powders, and the electrical resistivity of the structural components were analysed. The mixing ratio of 8Y and 3Y was kept at 1:1 by weight.

2. Experimental procedures

The large spherical granules of the 8Y and 3Y raw powders had a diameter of about 50 μm ; as shown in figure 1; they were an agglomeration of very fine crystallites. Two single-phase specimens and four mixed-phase specimens were designed. The two single-phase specimens, 8YS and 3YS, were made using 8Y and 3Y powder, respectively. They were fabricated by powder compaction under a 0.5 ton cm^{-2} compacting pressure. They provided the base-line property for the other mixed-phase microstructures. Their microstructures were composed of bulk and grain boundaries, but no phase boundaries. Here a grain boundary was defined

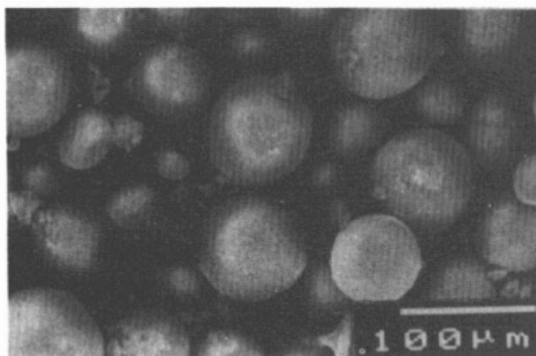


Figure 1. SEM photograph of ZrO_2 raw powders doped with Y_2O_3 .

as the boundary either between an 8Y grain and an 8Y grain or between a 3Y grain and a 3Y grain while a phase boundary was defined as the boundary between a 8Y grain and a 3Y grain.

Among the four mixed-phase specimens, two layered specimens had alternate layers of 8Y and 3Y and were denoted Par (parallel) and Ser (serial) according to the layer orientation with respect to the electrodes. The layer thickness was very large compared with the crystallite size. These specimens were composed of the bulk, many grain boundaries and a small number of phase boundaries at the interfaces between the layers. Par and Ser specimens were prepared by a conventional tape-casting process using a non-aqueous medium [11]. Slurries of 8Y and 3Y were cast into thin tapes and the tapes were multilayered.

Two mixed-phase specimens, one coarsely mixed specimen denoted GG (granule-granule) and the other finely mixed specimen denoted CC (crystallite-crystallite), were prepared by mixing 8Y and 3Y phases. The GG specimen was a homogeneous mixture of 8Y and 3Y coarse granules. In the microstructure of the CC specimen, fine crystallites of 8Y and 3Y were homogeneously dispersed. In these specimens a large number of phase boundaries existed. The GG specimen was produced by mixing the granular raw powders by shaking by hand and then compacted into discs like the 8YS and 3YS specimens. The CC specimen was made by disintegrating the two granular raw powders into a fine crystallite mixture by hard ball milling in alcohol for 72 h.

All the specimens were of a round or square shape of about 7 mm diameter or side. All these specimens were sintered at 1500 °C for 2 h in air. After sintering, a Pt paste was smeared on two flat surfaces of the specimens and baked at 1000 °C for 30 min in air. The electrical properties of the specimens were measured at 250, 450 and 750 °C in air using an impedance analyser (Hewlett-Packard 4192A) from 5 Hz to 13 MHz. The contributions of the microstructural components, i.e. the bulk and boundaries, to the electrical resistivities were analysed. Phases were identified by the x-ray diffraction method. Photographs and graphical expressions of the designed microstructures are displayed in figure 2.

3. Results and discussion

During the sintering, the 8Y phase showed a much higher rate of grain growth than 3Y. The grain size of 8Y in 8YS was about 10 μm while that of 3Y in 3YS was less than 1 μm .

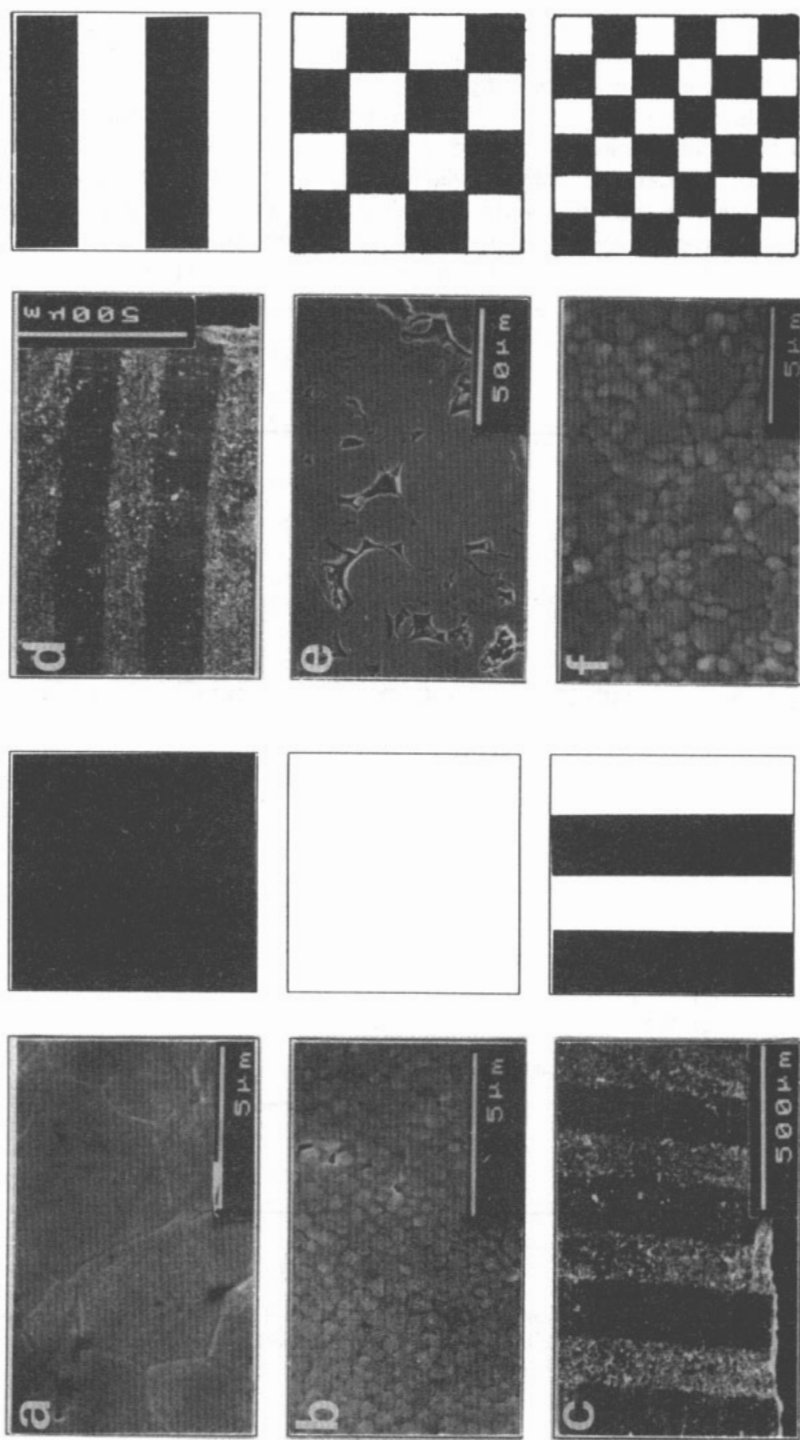


Figure 2. Photographs and graphical expressions for the designed microstructures: (a) 8Y; (b) 3Y; (c) Par; (d) Ser; (e) GG; (f) CC (see text).

However, in the CC specimen, the growth of 8Y grains was influenced by the presence of the slow-growing 3Y phase; so the grain size of the 8Y phase became a little smaller than in the 8YS specimen, as shown in figure 1.

X-ray diffraction analyses revealed that all specimens were composed of cubic and tetragonal ZrO_2 phases, as shown in figure 3. Figure 4 represents a Cole-Cole plot obtained by the complex impedance analyses where the Z axis is real and the X axis is imaginary. The first semicircle from the origin displays the properties of the bulk component while the second semicircle those of the grain boundary component [12]. The intersections of the semicircles with the Z axis allow the resistivity of the components to be determined. In the present work the arc of the semicircles were extrapolated to the Z axis and then the intersections were obtained.

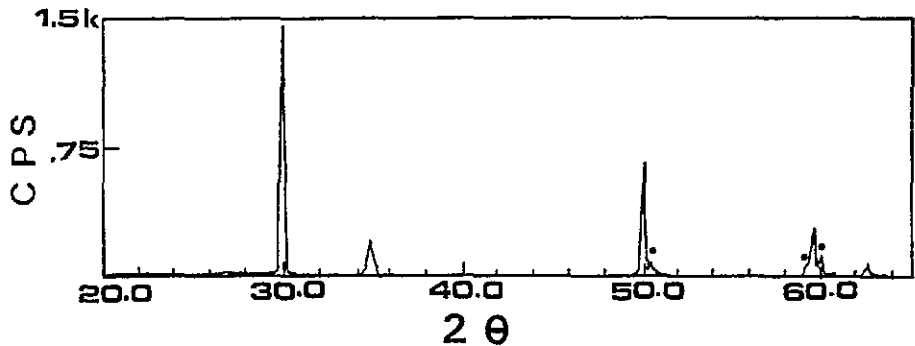


Figure 3. X-ray diffraction pattern of a mixed-phase specimen: ●, peaks representing the tetragonal phase only.

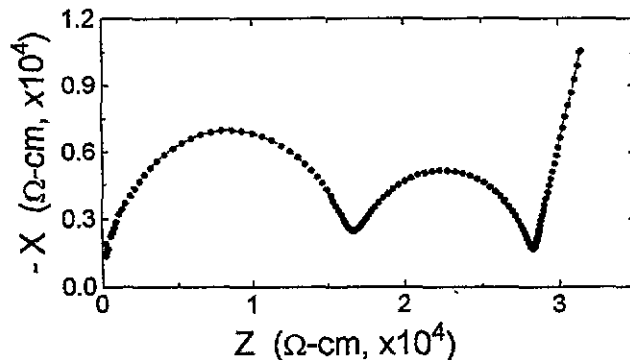


Figure 4. A representative Cole-Cole plot obtained by complex impedance analyses where the Z axis is real while the X axis is imaginary. The frequency increases from 5 Hz to 13 MHz approaching the origin.

The bulk and boundary resistivities measured at 250°C are depicted in figure 5. The height of each column roughly represents the total resistivity of the specimen. The resistivity of the bulk component of 8YS was higher than that of 3YS. The mixed-phase specimens had

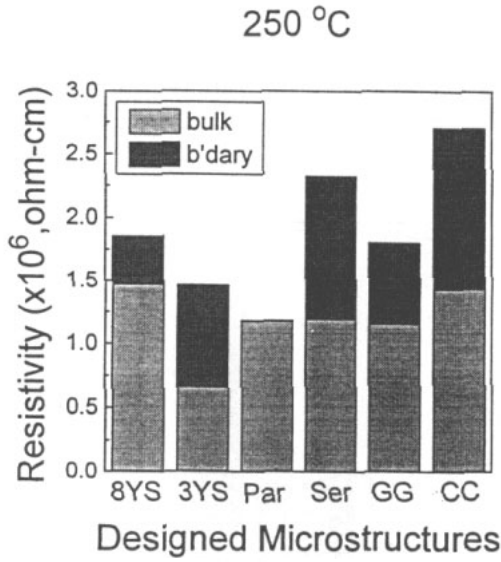


Figure 5. Electrical resistivities of the designed microstructures measured at 250 °C.

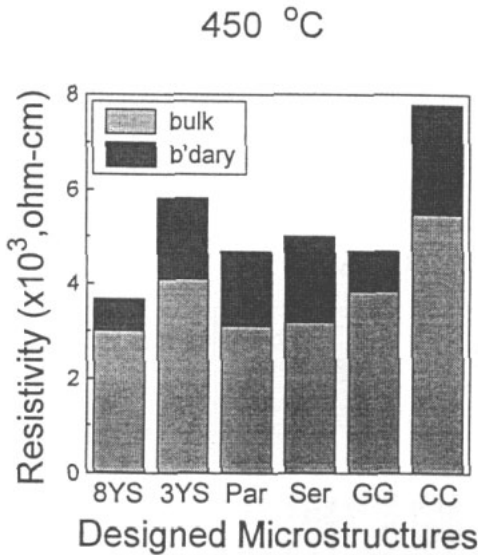


Figure 6. Electrical resistivities of the designed microstructures measured at 450 °C.

bulk resistivities located between the base-line values. They roughly satisfied the mixing rule. The resistivities of the boundary component were relatively high at this temperature.

At 450 °C, 8YS conversely showed a little lower bulk resistivity than 3YS, as shown in figure 6. The bulk resistivities of the other mixed-phase specimens are between the base-line values, except for the CC specimen. Compared with those at 250 °C, the contribution of the bulk component to the total resistivity was pronouncedly enhanced at this temperature while the influence of the boundary component was evidently reduced.

The resistivities measured at 750°C could no longer be divided into those of the structural components. In the high-temperature region, the total resistivity became dominated by that of bulk component. Compared with 8YS, the 3YS specimen exhibited a very high resistivity, as shown in figure 7. The bulk resistivities of the mixed-phase specimens were still between the base-line values again, except for the CC specimen.

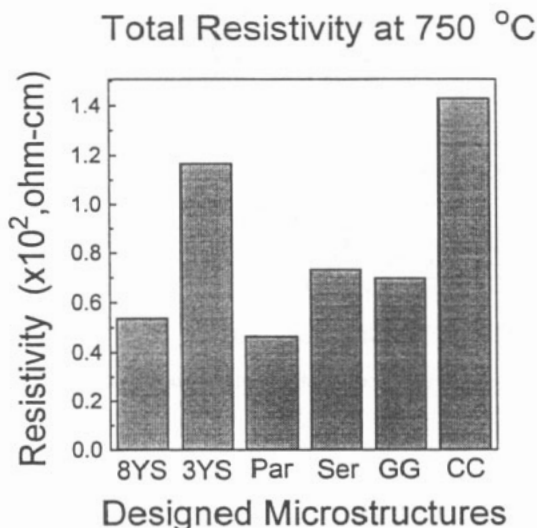


Figure 7. Electrical resistivities of the designed microstructures measured at 750°C.

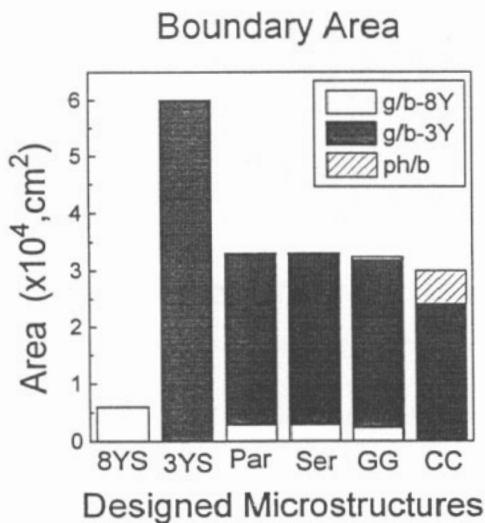


Figure 8. Estimated boundary areas of the designed microstructures: g/b-8Y, boundaries between 8Y and 8Y grains; g/b-3Y, boundaries between 3Y and 3Y grains; ph/b, boundaries between 8Y and 3Y grains.

The microstructures of the present work can be classified into three groups: the 8YS and 3YS group, the Par and Ser group, and the GG and CC group. 8YS had a higher bulk resistivity than 3YS in the low-temperature region, as reported by Badwall *et al* [13] but, at high temperatures, 8YS showed a much lower bulk resistivity than 3YS. The aging of partially stabilized zirconias resulted in an increase in bulk resistivity as the tetragonal-to-monoclinic transformation occurred [14]. In terms of the boundary resistivity, 3YS always displayed a larger resistivity than 8YS. However, if the grain boundary area is considered, the grain boundary area between 3Y grains seemed to be more conductive than the grain boundary area between 8YS grains.

Par and Ser specimens were different from each other in terms of the orientation to the electrodes. The Par specimen always demonstrated a lower resistivity than the Ser specimen because a low-resistivity electrical path could always be maintained (at least partially) in the Par overall electrical conduction in the Ser specimen. Both Par and Ser specimens displayed nearly the same bulk resistivity at low temperatures, but the boundary resistivity was relatively larger at 250°C for the Ser specimen than for the 8YS and 3YS specimens. This seemed to be the result of thin phase boundaries located perpendicular to the conduction direction. At high temperatures where the boundary was not important, the Ser specimen showed a lower resistivity than 3YS.

Although both of GG and CC specimens had a particulate mixed structure of 8Y and 3Y phases, the particle sizes of the GG specimen and the CC specimen were dissimilar. In the CC specimen every 8Y crystallite was surrounded by small 3Y crystallites; so there were a large number of phase boundaries but no 8Y grain boundaries. The CC specimen always exhibited higher resistivities of both the bulk and the boundaries than GG did. These high resistivities seemed to result in the presence of a large phase boundary area.

The mixed-phase specimens showed a bulk resistivity located mostly between the baseline values, except those of the CC specimen at 450 and 750°C. This meant that no severe change occurred in the bulk properties as a result of these microstructural designs. The high bulk resistivity of the finely mixed CC specimen might be the result of chemical impurities accumulated at the phase boundaries between the 3Y and 8Y phases, but this needs to be investigated further.

The boundary areas of the specimens were estimated by calculating the microstructural scales and are depicted in figure 8. Although the grain boundaries of the 3Y phase were dominant in all mixed-phase specimens, the phase boundary areas were apparently different for the various microstructures. The largest phase boundary area appeared in the CC specimen.

As there is a high boundary resistivity in the low-temperature region and a large phase boundary area in the CC specimen, the phase boundaries seem to play an important role in the electrical resistivity. It has already been reported that the boundary resistivity of ZrO_2 ceramics is very sensitive to the presence of impurities [9]. In the present work, impurities might have segregated to the phase boundaries during sintering or might have been introduced during the preparation processes. The phase boundary property itself has to be investigated further.

4. Conclusions

The electrical resistivity was markedly influenced by microstructural design in Y_2O_3 -stabilized ZrO_2 ceramics. 8YS specimens had a lower resistivity than 3YS specimens did. Compared with these single-phase specimens, the mixed-phase specimens composed of 8Y

and 3Y exhibited higher boundary resistivities. Grain boundaries and phase boundaries raised the electrical resistivity of the materials and played an important role at low temperatures, while the bulk resistivity dominated the total resistivity at high temperatures. The contribution of boundary component was apparent in the mixed-phase specimen, especially when a large number of phase boundaries existed.

Acknowledgments

The authors very much appreciated the experimental assistance of Messrs S J Oh and K H Kim and the helpful discussions of Dr I H Kuk.

References

- [1] Bauer E and Preis H 1937 *Z. Elektrochem.* **43** 727
- [2] Weissbart J and Ruka R 1962 *J. Electrochem. Soc.* **109** 723
- [3] Mori M and Asakawa C 1990 Solid Oxide Fuel Cells Report CRIEPI-R-EW90002, Japan
- [4] Philips S V and Datta A K 1990 *Proc. Conf. on Ceramics in Energy Applications* Session 3B, p 183
- [5] Schoonman J, Dekker J P and Broers J W 1991 *Solid State Ion.* **46** 299
- [6] Isenberg A O 1981 *Solid State Ion.* **3-4** 431
- [7] Gupta T K, Bechtold J H, Kuznicki R C, Cadoff L H and Rossing B R 1977 *J. Mater. Sci.* **12** 2421
- [8] Claussen N 1984 *Science and Technology of Zirconia II* ed N Claussen, R Rühle and A H Heuer (Columbus, OH: American Ceramic Society) p 325
- [9] Butler E P, Slotwinski R K, Bonanos N, Drennan J and Steele B C H 1984 *Science and Technology of Zirconia II* ed N Claussen, M Rühle and A H Heuer (Columbus, OH: American Ceramic Society) p 572
- [10] Kim S J, Kim K H, Oh S J, Kang T K and Kuk I H 1993 *J. Korean Ceram. Soc.* **30** 717
- [11] Shanefield D J and Mistler R E 1971 *West Electr. Eng.* **15** 15
- [12] Bauerle J E 1969 *J. Phys. Chem. Solids* **30** 2657
- [13] Badwal S P S, Ciacchi F T and Hannink R H J 1990 *Solid State Ion.* **40-1** 882
- [14] Slotwinski R K, Bonanos N, Steele B C H and Butler E P 1982 *Engineering with Ceramics* vol 32, ed R W Davidge (Stoke-on-Trent: British Ceramic Society) p 41